Mechanism of TRIM25 Catalytic Activation in the Antiviral RIG-I Pathway

Jacint G. Sanchez[1], **Jessica J. Chiang**[2], **Konstantin M.J. Sparrer**[3], **Steven L. Alam**[4], **Michael Chi**[1], **Marcin D. Roganowicz**[1], **Banumathi Sankaran**[5], **Michaela U. Gack**[2,3,*], and **Owen Pornillos**[1,*]

[1]Department of Molecular Physiology and Biological Physics, University of Virginia, Charlottesville, VA 22908, USA

[2]Department of Microbiology and Immunobiology, Harvard Medical School, Boston, MA 02115, USA

[3]Department of Microbiology, University of Chicago, Chicago, IL 60637, USA

[4]Department of Biochemistry, University of Utah, Salt Lake City, UT 84112, USA

[5]Molecular Biophysics and Integrated Bioimaging, Berkeley Center for Structural Biology, Lawrence Berkeley National Laboratory, Berkeley, CA 94720, USA

SUMMARY

Antiviral response pathways induce interferon by higher-order assembly of signaling complexes called signalosomes. Assembly of the RIG-I signalosome is regulated by K63-linked polyubiquitin chains, which are synthesized by the E3 ubiquitin ligase, TRIM25. We have previously shown that the TRIM25 coiled-coil domain is a stable, antiparallel dimer that positions two catalytic RING domains on opposite ends of an elongated rod. We now show that the RING domain is a separate self-association motif that engages ubiquitin-conjugated E2 enzymes as a dimer. RING dimerization is required for catalysis, TRIM25-mediated RIG-I ubiquitination, interferon induction, and antiviral activity. We also provide evidence that RING dimerization and E3 ligase activity are promoted by binding of the TRIM25 SPRY domain to the RIG-I effector domain. These results indicate that TRIM25 actively participates in higher-order assembly of the RIG-I signalosome and helps to fine-tune the efficiency of the RIG-I-mediated antiviral response.

*Correspondence: mgack@uchicago.edu (M.U.G.), opornillos@virginia.edu (O.P.).

INTRODUCTION

Higher-order assembly of large protein complexes is a recognized signal amplification mechanism that operates in many cellular signaling pathways (Wu, 2013). In the innate immune system, filamentous assemblies of the mitochondrial protein, MAVS (also known as CARDIF, VISA, or IPS-1), comprise one such type of signalosome (reviewed by Cai and Chen, 2014). MAVS filaments amplify signals from RIG-I-like pattern recognition receptors bound to viral RNA and recruit downstream effectors that ultimately generate a type I interferon (IFN) response. IFN-α/β gene expression induced by the RIG-I/MAVS signaling axis suppresses the replication of a variety of clinically important viral pathogens, including influenza A virus (IAV), hepatitis C virus, and dengue virus (reviewed by Goubau et al., 2013 and Loo and Gale, 2011).

Recent studies have shown that RIG-I-induced MAVS filament formation requires a remarkably simple biochemical trigger: interaction of the amino-terminal CARD (caspase activation and recruitment domain) of MAVS with a tetrameric assembly of the amino-terminal tandem CARDs (2CARD) of RNA-bound RIG-I (Jiang et al., 2012; Peisley et al., 2014; Wu et al., 2014). The RIG-I 2CARD tetramer is a helix with a single CARD as repeat unit, and so the 2CARD architecture restricts it to a "lock washer" configuration with only two helical turns (Peisley et al., 2014). The 2CARD "lock washer" acts as a template or seed for the single CARD of MAVS, which assembles along the helical trajectory to form long filaments containing several hundreds of MAVS CARD molecules (Peisley et al., 2014; Wu et al., 2014; Xu et al., 2014). MAVS filaments behave like prion fibers and thus are thought to commit the RIG-I pathway to an all-or-none or digital response to viral infection (Cai et al., 2014; Cai and Chen, 2014; Hou et al., 2011). Uncontrolled MAVS assembly will have harmful consequences to the cell, and so a number of mechanisms have evolved to regulate where, when, and how the RIG-I 2CARD seeds MAVS CARD assembly (reviewed by Chiang et al., 2014).

Ubiquitin (Ub) is a well-characterized regulator of the RIG-I 2CARD/MAVS CARD seeding mechanism (Gack et al., 2007, 2008; Jiang et al., 2012; Peisley et al., 2013, 2014; Zeng et al., 2010). Activated 2CARD is modified with K63-linked polyubiquitin chains (K63-polyUb) (Gack et al., 2007), and unanchored K63-polyUb chains were also shown to associate with RIG-I in biochemical reconstitution studies (Jiang et al., 2012; Zeng et al., 2010). Structural and biochemical studies have revealed that these K63-polyUb chains can wrap around four RIG-I 2CARD molecules to induce and stabilize the "lock washer" configuration (Jiang et al., 2012; Peisley et al., 2014). Both types of K63-polyUb chains are synthesized by the E3 ubiquitin ligase, TRIM25, which is an essential component of the RIG-I pathway (Gack et al., 2007; Zeng et al., 2010).

TRIM25 belongs to the tripartite motif (TRIM) protein family, which is characterized by a conserved domain organization at the N terminus (known as the TRIM or RBCC motif) composed of a catalytic RING domain, one or two B-box domains, and a coiled-coil dimerization domain (Meroni and Diez-Roux, 2005; Figure 1A). In addition, TRIM25 has a C-terminal SPRY domain that binds to the RIG-I 2CARD (D'Cruz et al., 2013; Gack et al., 2007, 2008). TRIM proteins, like the well-characterized cullin ligases, are modular E3

enzymes. Similar to the cullin scaffold, the TRIM coiled-coil domain defines the spatial disposition of the catalytic and substrate-binding/recruitment domains. The coiled-coil domain of TRIM25 makes an elongated, antiparallel dimer of hairpin-shaped subunits, which positions two RING domains on opposite ends of a 170-Å-long rod (Sanchez et al., 2014; Figure 1B). In the TRIM25 dimer, two C-terminal SPRY domains emanate from a four-helix bundle in the middle of the coiled coil. The SPRY domains are located on the same side of the dimer, which presumably allows them to simultaneously engage two substrate molecules (Goldstone et al., 2014; Li et al., 2014; Sanchez et al., 2014; Weinert et al., 2015). Cooperation between the catalytic and substrate-binding domains is likely facilitated by flexible linkers connecting these domains to the coiled-coil scaffold.

TRIM25 is recruited by RIG-I when RNA recognition by the helicase and C-terminal domains of RIG-I releases the 2CARD from autoinhibition (Jiang and Chen, 2011; Kowalinski et al., 2011; Luo et al., 2011), and the exposed 2CARD binds to the C-terminal SPRY domain of the E3 enzyme (D'Cruz et al., 2013; Gack et al., 2007, 2008). It is not known whether 2CARD binding is simply a mechanism to localize an already active ligase (and therefore K63-polyUb) to sites of seed or signalosome assembly or whether such localization is coupled to TRIM25 catalytic activation. Here, we use structural, biochemical, and cell biological approaches to analyze the mechanism of catalytic activation of TRIM25. We found that the RING domain constitutes a self-association motif that dimerizes to engage Ub-conjugated E2 enzymes and synthesize K63-pol-yUb. Because the two RING domains in the stable, coiled-coil-mediated TRIM25 dimer cannot self-associate and are effectively monomeric, our results imply that K63-polyUb synthesis is enabled only upon further, higher-order oligomerization of TRIM25. This is likely to be a quality control mechanism in the RIG-I pathway that couples TRIM25 catalytic activation to Ub-dependent 2CARD seed formation and MAVS assembly.

RESULTS

Structure of the TRIM25 RING Domain in Complex with E2-Ub

The antiparallel architecture of the TRIM25 coiled-coil dimerization domain implies that the associated RING domains are separated by about 170 Å and so are effectively monomeric in this context (Figure 1B). Indeed, the TRIM25 RING was proposed to act as a monomer, similar to the CBL-B RING domain (Li et al., 2014). Nevertheless, many more RING domains engage E2 enzymes as dimers, as exemplified by the non-TRIM E3 ligases, RNF4 and BIRC7. Structures of these proteins, each bound to a covalent E2-Ub conjugate, have been demonstrated to represent the catalytically primed form of these enzymes (Dou et al., 2012; Plechanovová et al., 2012). We therefore reasoned that, if the TRIM25 RING domain catalyzes K63-polyUb synthesis as a dimer, then its crystal structure with the relevant E2-Ub should reveal an equivalent quaternary fold—including high-resolution details—as the RNF4 and BIRC7 complexes.

To facilitate structure determination, we first identified E2-conjugating enzymes suitable for such analysis. Two Ubc5 isoforms (Ubc5b and Ubc5c; also known as Ube2D2 and Ube2D3, respectively) and Ubc13 (also known as Ube2N) have been previously shown to function in the RIG-I pathway (Liu et al., 2013; Zeng et al., 2009, 2010). Accordingly, we found that the

isolated RING domain of TRIM25 (residues 1–83) efficiently synthesized polyUb with these E2 enzymes (Figures 1C and S1); however, K63-polyUb chains were most efficiently made in vitro with Ubc13 and its partner, Uev1A (also known as Ube2V1; Figures 1D and 1E). Likewise, full-length TRIM25 is active with these E2 enzymes (Figure 1F). Interestingly, full-length TRIM25 predominantly made anchored Ub chains (autoubiquitination) with Ubc5b or Ubc13 alone and, conversely, only unanchored chains with Ubc13/Uev1A.

We were successful in co-crystallizing the TRIM25 RING domain with Ub-conjugated Ubc13 (Figure 2; Table S1). To prevent loss of the Ub moiety during crystallization, we used the previously described strategy of stably conjugating Ub to the E2 via an isopeptide linkage (Plechanovová et al., 2012) to make Ubc13^{C87K}-Ub. The structure of the TRIM25 RING/ Ubc13^{C87K}-Ub complex was determined to 2.4- Å resolution (R/R_{free} = 0.19/0.23).

Although the isolated TRIM25 RING domain is predominantly a monomer in solution (Figure S2A), it crystallized as a dimer in complex with Ubc13-Ub. This indicated that high-protein concentrations during crystallization and binding of Ubc13-Ub promoted dimerization of the RING domain. The TRIM25 RING/ Ubc13-Ub complex is strikingly similar to the RING/E2-Ub complexes of RNF4 and BIRC7 (Dou et al., 2012; Plechanovová et al., 2012; Figures 2A and 2B). Each RING domain interacts with Ubc13-Ub through an extensive three-way interface. TRIM25 Arg54 coordinates an extensive hydrogen bond network that packs the Ub C-terminal tail against a shallow groove leading to the E2 active site (Figure 2C), and the zinc-bound His30 side chain makes a hydrogen bond with the Ub Glu32 carbonyl (Figure 2D). These interactions help hold Ub in the so-called "closed" conformation primed for catalysis (Dou et al., 2012; Plechanovová et al., 2012; Pruneda et al., 2012). Complex formation also induces allosteric remodeling of the E2 active site, with the Ubc13 Asn79 side chain amide making a hydrogen bond with the isopeptide (normally thioester) carbonyl and the Asp119 side chain positioned to activate the incoming lysine nucleophile (Figure 2C). Furthermore, the Ub moiety also makes hydrogen bonds with the second RING, involving RING side chains Glu22, Lys65, and Asn71; Ub backbone carbonyls; and the Ub Asp32 side chain (Figure 2D). These high-resolution structural details are very similar, and in many aspects identical, to the previously described RING/E2-Ub complexes of RNF4 (Plechanovová et al., 2012) and BIRC7 (Dou et al., 2012; Figures 2B–2D). The striking equivalence of the three structures strongly indicates that TRIM25 engages E2-Ub conjugates as a dimer.

TRIM25 RING Dimerization Is Required for Polyubiquitin Synthesis In Vitro

The TRIM25 RING domain dimer is mediated by two regions of contact (Figure 3A). Thr25, Asn31, and Asn66 from the zinc-binding lobes coordinate a buried hydrogen bond network, which is contiguous with the hydrophilic interactions at the RING/E2-Ub interface. A small four-helix bundle formed by residues that flank the zinc lobes in primary sequence also stabilizes the dimer via buried aliphatic side chains (Leu7, Leu11, Val68, Leu69, and Val72). The TRIM25 RING dimer is therefore reminiscent of the BRCA1/BARD1 heterodimer, in that helical elements outside the main zinc cores also mediate dimer formation (Brzovic et al., 2001). To validate the structure, we systematically substituted alanine for residues buried in both regions of the TRIM25 dimer interface and then purified

the mutants (Figure 3B) and tested their catalytic activity (Figure 3C). Results showed that the RING mutants were invariably deficient in catalysis, with L69A and V72A showing the greatest deficiency (Figure 3C). Importantly, the size-exclusion profiles of all the RING mutants were similar to that of the wild-type protein, indicating that the mutants were also monomeric on purification and that none of the mutations affected the tertiary fold of the domain (Figure S3A). Similarly, the L69A and V72A mutations did not affect folding or the basal oligomerization of full-length TRIM25 (Figure S3B).

RING dimerization facilitates Ub conjugation because the two RING domains cooperate in holding the Ub moiety in a configuration primed for catalysis (Dou et al., 2012; Plechanovová et al., 2012). The first RING interacts with both E2 and Ub using a conserved set of interactions (Figures 2C and 2D), whereas the second RING contacts the same Ub using a different set of non-conserved residues (Figure 2D). In RNF4 and BIRC7, the second set of interactions primarily consists of pi-stacking between a Ub backbone peptide and a tyrosine or phenylalanine side chain (Figure 2D, middle and bottom panels; Dou et al., 2012; Plechanovová et al., 2012). In contrast, the TRIM25 interface consists of a hydrogen bond network mediated in part by Lys65 and Asn71 (Figures 2D, top panel, and 4A). To confirm that this set of interactions is important for catalysis, we also generated the K65A, N71A, and N71D mutants (Figure 4B) and assayed them for ubiquitination activity (Figure 4C). Although the N71A mutant was still catalytically active, both the K65A and N71D mutants were severely deficient. Thus, like RNF4 and BIRC7, the second set of RING/Ub interactions is also required for TRIM25 catalytic activity.

In summary, the results of our structure-based mutagenesis experiments support the conclusion that the TRIM25 RING domain is catalytically active as a dimer. This has now been further confirmed by an independent structure of the TRIM25 RING domain in complex with Ubc5a-Ub, which was reported while this paper was under review (Koliopoulos et al., 2016). The TRIM5α RING domain in complex with unconjugated Ubc13 is also a dimer (Yudina et al., 2015), as are uncomplexed structures of TRIM37 (PDB 3LRQ) and TRIM32 (Koliopoulos et al., 2016), and so this may be a general property of the TRIM family of E3 ligases.

TRIM25 RING Dimerization Is Required for RIG-I Signaling

Our structural and biochemical analyses identified the RING domain as a second self-association motif in TRIM25, in addition to the coiled-coil dimerization motif. We therefore sought to examine the requirement for both types of interactions in promoting RIG-I-mediated signaling. To test the signal-transducing activities of wild-type (WT) and mutant TRIM25 proteins without potentially confounding effects by the presence of endogenous TRIM25 protein, we utilized CRISPR technology to generate *TRIM25*-knockout (KO) HEK293T cells (Figure S4A; see Supplemental Experimental Procedures for details). Immunoblot (IB) analysis confirmed the absence of endogenous TRIM25 protein in these cells (Figure S4B). To further validate the *TRIM25*-KO cells, we tested them for their ability to support RIG-I 2CARD-mediated IFN-β promoter activation by a luciferase assay (Figure S4C). As previously shown (Gack et al., 2007), glutathione-S-transferase (GST)-fused RIG-I 2CARD (GST-2CARD) potently induced IFN-β promoter activation in normal (WT)

HEK293T cells due to its constitutive signal-inducing activity. In contrast, IFN-β promoter activation induced by GST-2CARD was very low in *TRIM25*-KO cells (Figure S4C). Consistent with these results, an IAV infection assay showed low viral NS1 protein expression in WT cells, indicative of well-controlled virus replication (Figure S4D). In contrast, the expression of IAV NS1 protein was high in the *TRIM25*-KO cells, indicating that these cells are impaired in suppressing virus replication.

To determine the signal-promoting activity of TRIM25 mutants, we performed the IFN-β luciferase assay in *TRIM25*-KO cells that have been transfected with GST-2CARD together with two different amounts (1 or 5 ng) of plasmid encoding WT or structure-based mutants of TRIM25. As previously shown (Gack et al., 2007), WT TRIM25 strongly enhanced GST-2CARD-mediated signaling in a dose-dependent manner (Figure 5A). In striking contrast, TRIM25 mutants harboring the L69A and V72A mutations, which disrupted the RING dimer interface, did not potentiate 2CARD-mediated signaling; that is, IFN-β promoter activation induced by GST-2CARD co-expressed with TRIM25 L69A or V72A was similar to that of GST-2CARD expressed alone. The lack of IFN-β-inducing activity of the TRIM25 L69A and V72A mutants correlated very well with loss of ubiquitination of the RIG-I 2CARD (Figure 5B), confirming that the abolished signal-promoting activity of TRIM25 L69A and V72A is due to defective E3 ligase activity.

We also tested TRIM25 proteins harboring Y245A and L252A mutations, which severely disrupted dimerization of the isolated coiled-coil domain (Sanchez et al., 2014). These TRIM25 mutants showed only slightly reduced activities in promoting GST-2CARD-mediated IFN-β promoter activation as compared to WT TRIM25 at higher expression, whereas they had similar activities to WT TRIM25 at low expression (Figure 5A). The TRIM25 coiled-coil mutants also supported GST-2CARD ubiquitination, although this was somewhat reduced compared to WT TRIM25, in particular for the L252A mutant (Figure 5B).

To determine the antiviral activity of TRIM25 mutants with disrupted RING dimer (L69A or V72A) or coiled-coil dimer (Y245A or L252A) interfaces, we reconstituted *TRIM25*-KO cells with the individual mutants and subsequently infected them with IAV. Cells transfected with empty vector or WT TRIM25 served as controls (Figures 5C and 5D). Cells reconstituted with WT TRIM25 potently inhibited viral titers (by more than four log) and viral NS1 protein expression as compared to cells reconstituted with empty vector (Vec). In contrast, cells reconstituted with the TRIM25 L69A or V72A mutant had similar viral titers and NS1 protein levels as vector-complemented cells, indicating a profound defect in antiviral activity of these TRIM25 mutants. Furthermore, cells reconstituted with the Y245A and L252A mutants showed only a slightly reduced antiviral activity as compared to WT TRIM25 (Figures 5C and 5D), which is consistent with the IFN-β luciferase and 2CARD ubiquitination data (Figures 5A and 5B).

The modest defect caused by the Y245A and L252A coiled-coil dimerization mutations was somewhat surprising, because these mutations resulted in severe misfolding of the isolated coiled-coil domain of TRIM25, as determined by a thermal melting assay (Sanchez et al., 2014). We therefore tested the effect of these mutations on the thermal melting profile of

full-length TRIM25. In contrast to the isolated coiled-coil mutant proteins, the full-length mutants were more easily purifiable and remained dimeric, although, as expected, they were less stable than WT (Figure S5). Thus, the folding defect caused by Y245A and L252A was much less pronounced in context of full-length TRIM25, explaining the modest effect of these mutations in the cell-based assays. We surmise that the presence of eukaryotic chaperones during expression of the full-length mutants likely compensates for the folding and dimerization defect caused by the coiled-coil mutations.

Analysis of TRIM25 Self-Association in Solution

The above results indicated that the stable, coiled-coil-mediated TRIM25 dimer (Sanchez et al., 2014) is insufficient for catalysis and that engagement of the E2-conjugating enzyme and polyUb synthesis occurs with further, higher-order assembly of the ligase. Indeed, TRIM5α, another antiviral TRIM family member, becomes catalytically active precisely by this mechanism. Higher-order assembly of TRIM5α is mediated by its single B-box domain, which facilitates spontaneous assembly of coiled-coil-mediated TRIM5α dimers into an extended lattice (Diaz-Griffero et al., 2009; Ganser-Pornillos et al., 2011; Li and Sodroski, 2008; Li et al., 2016; Wagner et al., 2016). Note that, in contrast to TRIM5α, TRIM25 has a tandem of B-boxes (Figure 1A). To determine whether TRIM25 also assembles spontaneously in a B-box-dependent manner, we analyzed the solution behavior of full-length TRIM25 (Figures S2B and S2C). Notably, we found that full-length TRIM25 had significant E3 ligase activity at nanomolar concentrations (Figure 1F). This was in contrast to the isolated RING domain, which catalyzed polyUb formation only at micromolar concentrations (Figure 1C) and suggested that, in context of the full-length protein, RING-RING interactions occurred more readily. We have previously shown that the isolated coiled-coil domain of TRIM25 is a stable dimer in solution, and indeed, freshly purified full-length TRIM25 also behaved as a stable dimer at low-protein concentrations (Figure S2B). Interestingly, at higher concentrations, we reproducibly detected the presence of a minor species with molecular weight consistent with a tetramer (Figure S2C). However, extensive analysis by electron microscopy did not reveal convincing evidence of spontaneous higher-order or lattice-type assembly behavior for TRIM25. These results indicated that unlike the B-box 2 domain of TRIM5α, the equivalent domain in TRIM25 does not spontaneously self-associate. We conclude that efficient TRIM25 RING domain activation is likely to be facilitated by other factors.

RIG-I 2CARD Enhances TRIM25's Catalytic Activity In Vitro

What might be the factors that promote assembly of catalytically active TRIM25? Our data indicate that a minimum of two coiled-coil-mediated TRIM25 dimers (or four monomers) is required to generate a catalytically active E3 ligase. This matches the stoichiometry of the 2CARD tetramer that seeds MAVS filament assembly. Therefore, an appealing hypothesis is that TRIM25 and RIG-I mutually promote each other's oligomerization and activation. Indeed, it has been demonstrated that K63-linked poly-Ub chains synthesized by TRIM25 can promote 2CARD tetramerization in vitro (Peisley et al., 2014). We therefore performed the complementary experiment to ask whether 2CARD promotes higher-order oligomerization and catalytic activation of TRIM25.

We first titrated TRIM25 concentrations in our ubiquitination reactions and found that, with 100 nM of full-length TRIM25, poly-Ub chain formation was minimal with either Ubc13/Uev1A (Figure 6A, lane 3) or Ubc5c (Figure 6A, lane 7). The same reactions were then performed in the presence of 1 µM of freshly purified His-tagged 2CARD, and we found that polyUb synthesis was very significantly enhanced (Figure 6A, compare lane 4 to lane 3 and lane 8 to lane 7). Thus, RIG-I 2CARD can promote TRIM25 RING/RING self-association in vitro and, by implication, higher-order oligomerization of coiled-coil-mediated TRIM25 dimers.

To determine whether polyUb-mediated 2CARD tetramerization was required for this effect, we measured catalysis using a Ub discharge assay in which polyUb chains were not being made (Middleton et al., 2014). In this assay, E2-Ub conjugates were first synthesized by incubation of E1 and E2 enzymes with Ub and ATP. Discharge of the Ub moiety was then monitored by the disappearance of the E2-Ub conjugate and appearance of free E2, under conditions that prevent recharging of the E2. To slow down the reaction, we used oxyester-linked Ubc5b$^{S22R/C85S}$-Ub conjugates and did not add excess Ub acceptor amine (Middleton et al., 2014; Wright et al., 2016). In this assay format, we found that TRIM25 did not significantly increase the basal rate of free E2 accumulation, probably because dissociation of the RING/RING dimer or RING/E2-Ub complex was fast relative to oxyester cleavage. We then found that the presence of 2CARD also did not result in increased discharge (Figure 6B), even though we used a GST-2CARD fusion protein that was already dimeric due to the GST tag. On the other hand, when the added GST-2CARD was pre-incubated with K63-linked tetraUb, TRIM25-mediated discharge was increased. The effect was modest but was nevertheless evident, especially when comparing the initial time points (30–90 s), and was reproducibly observed in two independent experiments performed with independent protein preparations (Figure 6B). Because incubation with K63-linked polyUb chains induces 2CARD tetramerization in vitro (Peisley et al., 2014), these results indicated that the presence of the 2CARD tetramer also stabilized the TRIM25 RING dimer and/or RING/E2-Ub complexes, i.e., that 2CARD oligomerization and TRIM25 oligomerization can occur cooperatively.

Finally, we found that mutation of T55 in the first CARD, which is a critical residue for TRIM25 SPRY domain binding (Gack et al., 2008), did not increase TRIM25-mediated Ub discharge, even when the mutant GST-2CARD was pre-incubated with K63-linked polyUb (Figure 6B). This result confirmed expectation that RIG-I 2CARD-mediated TRIM25 activation is dependent on binding of 2CARD to the SPRY domain of TRIM25.

DISCUSSION

The essential role of TRIM25 in the RIG-I pathway is underscored by findings that viruses, such as IAV and dengue virus, have evolved mechanisms to suppress RIG-I signaling by specifically targeting and disrupting TRIM25 function (Gack et al., 2009; Manokaran et al., 2015; Rajsbaum et al., 2012). In this study, we confirm the essential requirement for TRIM25's E3 ubiquitin ligase activity in RIG-I signaling (Gack et al., 2007) by showing that mutations that disrupt TRIM25 RING domain activation also reduce to background levels the ubiquitination of RIG-I 2CARD, 2CARD-dependent IFN induction, and antiviral activity

against IAV. Furthermore, our results show that the TRIM25 RING domain must dimerize in order to productively engage Ub-conjugated E2 enzymes and become catalytically active, which is a common (but not universal) property of the RING family of E3 ubiquitin ligases (Lima and Schulman, 2012). Like other TRIM proteins, the basal oligomeric state of TRIM25 is a stable, coiled-coil-mediated dimer (Goldstone et al., 2014; Li et al., 2014; Sanchez et al., 2014; Weinert et al., 2015). The TRIM25 coiled-coil dimer has an antiparallel architecture, which places the two associated RING domains on opposite ends of an elongated rod (Sanchez et al., 2014). Therefore, TRIM25 RING dimers very likely form by means of higher-order oligomerization (or assembly) of the coiled-coil-mediated dimers.

We envision at least two possible types of assembled, catalytically active TRIM25: a tetramer form wherein one coiled-coil-mediated dimer would interact with a second to allow head-to-head interactions of their RING domains or a filamentous or net form wherein the RING domains on opposite ends of the coiled coil would interact with RING domains from separate dimers (Figure 7). TRIM5α, another well-characterized TRIM protein, makes higher-order complexes by the second mechanism; in this case, individual N-terminal RING domains are brought into close proximity by spontaneous trimerization of the downstream B-box 2 domains and assembly of TRIM5α dimers into an extended hexagonal network (Ganser-Pornillos et al., 2011; Li et al., 2016; Wagner et al., 2016; Yudina et al., 2015). Our analysis did not reveal a similar type of spontaneous high-order assembly behavior for TRIM25, indicating that its RING domains are brought into proximity by a different mechanism.

Initial recognition of viral RNA by RIG-I occurs at a tri- or di-phosphorylated blunt end of the viral RNA (Cui et al., 2008; Goubau et al., 2014; Hornung et al., 2006; Jiang and Chen, 2011; Kowalinski et al., 2011; Luo et al., 2011; Pichlmair et al., 2006). Multiple RIG-I molecules can decorate the same RNA (if it is of sufficient length) in an ATP-dependent manner (Peisley et al., 2013). This property of RIG-I is thought to promote clustering of activated 2CARDs, because a minimum of four 2CARD molecules is required to seed MAVS CARD filament assembly and initiate signaling (Peisley et al., 2014; Wu et al., 2014). We found that, at least in vitro, the isolated 2CARD can promote TRIM25 catalytic activation, in a manner that appears dependent on binding of 2CARD to the TRIM25 SPRY domain. These results indicate that RIG-I assembly on the viral RNA has the additional purpose of recruiting and clustering multiple TRIM25 dimers to activate K63-polyUb synthesis. Such a coupled recruitment and activation mechanism avoids any potential off-pathway effects of polyUb chains because these are synthesized only when needed and at the correct location.

Furthermore, we propose that mutually productive engagement of RIG-I and TRIM25 goes beyond simple proximity-induced self-association and activation. Because 2CARD-mediated enhancement of TRIM25 activity in vitro is also dependent on polyUb, it is very likely that formation of the tetrameric 2CARD seed is cooperative with TRIM25 RING dimerization and catalytic activation. Indeed, it is probable that there is an avidity component to the interaction, because a head-to-head TRIM25 tetramer should cluster four SPRY domains and allow simultaneous, stoichiometric SPRY/2CARD binding. A cooperative assembly mechanism is consistent with the finding that TRIM25, RNA-bound

RIG-I, and the chaperone protein 14-3-3ε make a stable ternary complex that translocates from the cytosol to mitochondria in order to activate MAVS (Liu et al., 2012).

In summary, our results help to explain why TRIM25 is an essential player in the RIG-I-signaling pathway. In addition to its role as an enzymatic effector of RIG-I, TRIM25 confers additional biochemical functionalities that promote 2CARD tetramerization and signal propagation. TRIM25 therefore helps to fine-tune the efficiency of RIG-I-mediated signaling to high degree, which is an important property that allows the pathway to respond effectively even if viral challenge is low.

EXPERIMENTAL PROCEDURES

Protein Expression and Purification

Detailed methods to purify proteins and characterize them by analytical ultracentrifugation and size exclusion chromatography and multi-angle light scattering (SEC-MALS) are described in Supplemental Experimental Procedures.

Ubiquitination Assay

E1 and E2 enzymes and Ub were either purified in house or purchased from Boston Biochem, UBPBio, or Enzo Life Sciences. Ubiquitination reactions were incubated at 37°C in 50 mM Tris (pH 7.5), 150 mM NaCl, 0.5 mM tris(2-carboxyethyl)phosphine (TCEP), or 1 mM β-mercaptoethanol and typically contained E1 (50 or 100 nM), E2 (280 nM Ubc13/Uev1A, 1 μM Ubc13, or 1 μM Ubc5b), E3 (200 nM TRIM25 or 5 μM RING), Ub (40 μM), ATP (3 mM), and $MgCl_2$ (5 mM). Reactions were stopped by addition of SDS-PAGE sample buffer and boiling for 10 min. Typically, time points were taken at 0, 5, and/or 20 min. Immunoblots were performed with anti-Ub (1:2,000; P4D1; Santa Cruz Biotechnology), K63-linkage-specific anti-Ub (1:1,000; Enzo Life Sciences), anti-pentaHis (1:1,000; QIAGEN), and anti-FLAG M2 (1:5,000; Sigma). Signals were detected with a fluorescent secondary antibody (Rockland) and a LI-COR Odyssey scanner.

Ubiquitin Discharge Assay

This assay was performed essentially as described (Wright et al., 2016). $Ubc5b^{S22R/C85S}$-Ub oxyester-linked conjugate was prepared by mixing the following: 200 μM Ubc5b, 300 μM Ub, 1 μM E1, 50 mM Tris (pH 7.5), 150 mM NaCl, 5 mM ATP, 5 mM $MgCl_2$, 0.5 mM TCEP, and 0.1% Triton X-100. After overnight incubation at 37°C, the E1 enzyme and free ATP were removed by gel filtration in 20 mM Tris (pH 7.5) and 150 mM NaCl. Fractions containing E2-Ub, free E2, and free Ub were collected and concentrated to 4 mg/ml (5× concentration). Discharge reactions containing 1× $Ubc5b^{S22R/C85S}$-Ub, 1 μM TRIM25, and 8 μM GST-2CARD (WT or T55D), with or without 5 μM K63-linked tetraUb (Boston Biochem) in 50 mM Tris (pH 7.5) and 50 mM NaCl were incubated at 37°C. Time points were taken every 30 min over 3 hr and quenched by addition of non-reducing SDS-PAGE and subsequent placement on ice. Reactions products were visualized by SDS-PAGE and Coomassie staining. Free $Ubc5b^{S22R/C85S}$ was quantified by using a LI-COR Odyssey scanner. The experiment was performed twice, each with freshly purified batches of TRIM25 and 2CARD.

Structure Determination of the TRIM25 RING/Ubc13-Ub Complex

The purified RING and Ubc13^{C87K}-Ub conjugate samples were diluted to 20 μM using their respective size exclusion buffers, mixed at equal volumes, and then concentrated to 10 mg/ml. Crystallization was performed in sitting drops with commercial screens at a 2:1 protein-to-precipitant ratio. Crystals formed in Hampton PEG/Ion HT Screen condition no. D9 (0.2 M Li citrate and 20% polyethylene glycol (PEG) 3,350) after 2 days and were used for data collection without optimization. Ethylene glycol (10% [v/v] in mother liquor) was used as cryoprotectant. Diffraction data collected at beamline 5.0.1 at the Advanced Light Source were indexed and scaled using HKL2000 (Otwinowski and Minor, 1997).

The phase problem was solved by molecular replacement with crystal structures of human Ubc13 (PDB 1J7D) and Ub (PDB 1UBQ). The Ubc13 active site loop and Ub tail were removed from the search models to obtain unbiased densities for these regions. After positioning of the Ubc13 and Ub moieties, rigid body refinement also revealed strong densities for the zinc atoms in the RING domains as well as coordinating side chains and associated loops. These served as guides for calculation of 2-fold noncrystallographic symmetry (NCS) averaged maps, which were used to build the RING domains. Iterative refinement and manual model building were performed with PHENIX (version 1.9-1692; Adams et al., 2010) and Coot (Emsley et al., 2010). Secondary structure, torsion angle NCS, covalent bond and angle restraints for the Ubc13 K87-Ub G76 isopeptide, and zinc coordination (bond and angle) restraints were applied during refinement. Structure validation tools (as implemented in PHENIX and Coot) were used throughout the refinement process. Structure statistics are summarized in Table S1.

Cell Culture

Plasmids and viruses, cell culture methods, and generation of *TRIM25*-KO HEK293T cells are described in Supplemental Experimental Methods.

IFN-β Luciferase Assay

TRIM25-KO HEK293T cells were seeded into 24-well plates. The next day, the cells were transfected with 100 ng of IFN-β luciferase reporter plasmid and 150 ng of β-galactosidase-expressing pGK-β-gal. To stimulate IFN-β promoter activity, cells were also transfected with 1 ng of plasmid encoding GST-2CARD together with 1 or 5 ng of empty pCMV vector or pCMV-FLAG-TRIM25 WT or mutant constructs. Twelve hours later, whole-cell lysates (WCLs) were prepared and subjected to a luciferase assay (Promega). Luciferase values were normalized to β-galactosidase activity to measure the transfection efficiency.

GST Pull-Down Assay and Immunoblot Analysis

Pelleted cells were lysed in NP-40 buffer (50 mM HEPES [pH 7.4], 150 mM NaCl, 1% [v/v] NP-40, and protease inhibitor cocktail [Roche]), followed by centrifugation at 13,000 rpm for 25 min. Lysates were mixed with a 50% slurry of glutathione-conjugated Sepharose beads (GE Healthcare), and the binding reaction was incubated for 3 hr at 4°C. Precipitates were washed extensively with lysis buffer. Proteins bound to the beads were separated by SDS-PAGE and transferred to a polyvinylidene difluoride (PVDF) membrane (Bio-Rad). Immunoblots were performed with anti-Ub (1:5,000; P4D1; Santa Cruz), anti-FLAG

(1:2,000; Sigma), anti-GST (1:2,000; Sigma), anti-RIG-I (1:1,000; Adipogen), anti-TRIM25 (1:2,000; BD Biosciences), anti-actin (1:5,000–1:15,000; Sigma), or anti-NS1 (polyclonal rabbit; 1:3,000; kindly provided by Adolfo García-Sastre, Mount Sinai). The proteins were visualized by a chemiluminescence reagent (Pierce) and detected with a GE Healthcare Amersham Imager.

Influenza Replication Assays

TRIM25-KO HEK293T cells, seeded into 12-well plates, were transfected with 2 μg of pCMV empty vector or pCMV-FLAG-TRIM25 WT or mutant constructs. At 24 hr post-transfection, cells were infected with IAV (MOI 0.01) for 96 hr. To determine viral titers, supernatants were subjected to an endpoint titration (TCID50) assay on MDCK cells in DMEM supplemented with Pen-Strep, 0.2% BSA (Sigma), 25 mM HEPES, and 2 μg/ml TPCK-trypsin (Worthington Biochemical), as described previously (Balish et al., 2013). Furthermore, cells were harvested and WCLs prepared and subjected to SDS-PAGE and IB analysis using anti-NS1, anti-FLAG, and anti-actin antibodies.

Supplementary Material

Refer to Web version on PubMed Central for supplementary material.

Acknowledgments

References

Adams PD, Afonine PV, Bunkóczi G, Chen VB, Davis IW, Echols N, Headd JJ, Hung LW, Kapral GJ, Grosse-Kunstleve RW, et al. PHENIX: a comprehensive Python-based system for macromolecular structure solution. Acta Crystallogr D Biol Crystallogr. 2010; 66:213–221. [PubMed: 20124702]

Balish AL, Katz JM, Klimov AI. Influenza: propagation, quantification, and storage. Curr Protoc Microbiol. 2013; 29:15G.1.1–15G.1.24.

Brzovic PS, Rajagopal P, Hoyt DW, King MC, Klevit RE. Structure of a BRCA1-BARD1 heterodimeric RING-RING complex. Nat Struct Biol. 2001; 8:833–837. [PubMed: 11573085]

Cai X, Chen ZJ. Prion-like polymerization as a signaling mechanism. Trends Immunol. 2014; 35:622–630. [PubMed: 25457352]

Cai X, Chen J, Xu H, Liu S, Jiang QX, Halfmann R, Chen ZJ. Prion-like polymerization underlies signal transduction in antiviral immune defense and inflammasome activation. Cell. 2014; 156:1207–1222. [PubMed: 24630723]

Chiang JJ, Davis ME, Gack MU. Regulation of RIG-I-like receptor signaling by host and viral proteins. Cytokine Growth Factor Rev. 2014; 25:491–505. [PubMed: 25023063]

Cui S, Eisenächer K, Kirchhofer A, Brzózka K, Lammens A, Lammens K, Fujita T, Conzelmann KK, Krug A, Hopfner KP. The C-terminal regulatory domain is the RNA 5′-triphosphate sensor of RIG-I. Mol Cell. 2008; 29:169–179. [PubMed: 18243112]

D'Cruz AA, Kershaw NJ, Chiang JJ, Wang MK, Nicola NA, Babon JJ, Gack MU, Nicholson SE. Crystal structure of the TRIM25 B30.2 (PRYSPRY) domain: a key component of antiviral signalling. Biochem J. 2013; 456:231–240. [PubMed: 24015671]

Diaz-Griffero F, Qin XR, Hayashi F, Kigawa T, Finzi A, Sarnak Z, Lienlaf M, Yokoyama S, Sodroski J. A B-box 2 surface patch important for TRIM5α self-association, capsid binding avidity, and retrovirus restriction. J Virol. 2009; 83:10737–10751. [PubMed: 19656869]

Dou H, Buetow L, Sibbet GJ, Cameron K, Huang DT. BIRC7-E2 ubiquitin conjugate structure reveals the mechanism of ubiquitin transfer by a RING dimer. Nat Struct Mol Biol. 2012; 19:876–883. [PubMed: 22902369]

Emsley P, Lohkamp B, Scott WG, Cowtan K. Features and development of Coot. Acta Crystallogr D Biol Crystallogr. 2010; 66:486–501. [PubMed: 20383002]

Gack MU, Shin YC, Joo CH, Urano T, Liang C, Sun L, Takeuchi O, Akira S, Chen Z, Inoue S, Jung JU. TRIM25 RING-finger E3 ubiquitin ligase is essential for RIG-I-mediated antiviral activity. Nature. 2007; 446:916–920. [PubMed: 17392790]

Gack MU, Kirchhofer A, Shin YC, Inn KS, Liang C, Cui S, Myong S, Ha T, Hopfner KP, Jung JU. Roles of RIG-I N-terminal tandem CARD and splice variant in TRIM25-mediated antiviral signal transduction. Proc Natl Acad Sci USA. 2008; 105:16743–16748. [PubMed: 18948594]

Gack MU, Albrecht RA, Urano T, Inn KS, Huang IC, Carnero E, Farzan M, Inoue S, Jung JU, García-Sastre A. Influenza A virus NS1 targets the ubiquitin ligase TRIM25 to evade recognition by the host viral RNA sensor RIG-I. Cell Host Microbe. 2009; 5:439–449. [PubMed: 19454348]

Ganser-Pornillos BK, Chandrasekaran V, Pornillos O, Sodroski JG, Sundquist WI, Yeager M. Hexagonal assembly of a restricting TRIM5α protein. Proc Natl Acad Sci USA. 2011; 108:534–539. [PubMed: 21187419]

Goldstone DC, Walker PA, Calder LJ, Coombs PJ, Kirkpatrick J, Ball NJ, Hilditch L, Yap MW, Rosenthal PB, Stoye JP, Taylor IA. Structural studies of postentry restriction factors reveal antiparallel dimers that enable avid binding to the HIV-1 capsid lattice. Proc Natl Acad Sci USA. 2014; 111:9609–9614. [PubMed: 24979782]

Goubau D, Deddouche S, Reis e Sousa C. Cytosolic sensing of viruses. Immunity. 2013; 38:855–869. [PubMed: 23706667]

Goubau D, Schlee M, Deddouche S, Pruijssers AJ, Zillinger T, Goldeck M, Schuberth C, Van der Veen AG, Fujimura T, Rehwinkel J, et al. Antiviral immunity via RIG-I-mediated recognition of RNA bearing 5′-diphosphates. Nature. 2014; 514:372–375. [PubMed: 25119032]

Hornung V, Ellegast J, Kim S, Brzózka K, Jung A, Kato H, Poeck H, Akira S, Conzelmann KK, Schlee M, et al. 5′-Triphosphate RNA is the ligand for RIG-I. Science. 2006; 314:994–997. [PubMed: 17038590]

Hou F, Sun L, Zheng H, Skaug B, Jiang QX, Chen ZJ. MAVS forms functional prion-like aggregates to activate and propagate antiviral innate immune response. Cell. 2011; 146:448–461. [PubMed: 21782231]

Jiang QX, Chen ZJ. Structural insights into the activation of RIG-I, a nanosensor for viral RNAs. EMBO Rep. 2011; 13:7–8. [PubMed: 22157887]

Jiang X, Kinch LN, Brautigam CA, Chen X, Du F, Grishin NV, Chen ZJ. Ubiquitin-induced oligomerization of the RNA sensors RIG-I and MDA5 activates antiviral innate immune response. Immunity. 2012; 36:959–973. [PubMed: 22705106]

Koliopoulos MG, Esposito D, Christodoulou E, Taylor IA, Rittinger K. Functional role of TRIM E3 ligase oligomerization and regulation of catalytic activity. EMBO J. 2016; 35:1204–1218. [PubMed: 27154206]

Kowalinski E, Lunardi T, McCarthy AA, Louber J, Brunel J, Grigorov B, Gerlier D, Cusack S. Structural basis for the activation of innate immune pattern-recognition receptor RIG-I by viral RNA. Cell. 2011; 147:423–435. [PubMed: 22000019]

Li X, Sodroski J. The TRIM5α B-box 2 domain promotes cooperative binding to the retroviral capsid by mediating higher-order self-association. J Virol. 2008; 82:11495–11502. [PubMed: 18799578]

Li Y, Wu H, Wu W, Zhuo W, Liu W, Zhang Y, Cheng M, Chen YG, Gao N, Yu H, et al. Structural insights into the TRIM family of ubiquitin E3 ligases. Cell Res. 2014; 24:762–765. [PubMed: 24722452]

Li YL, Chandrasekaran V, Carter SD, Woodward CL, Christensen DE, Dryden KA, Pornillos O, Yeager M, Ganser-Pornillos BK, Jensen GJ, Sundquist WI. Primate TRIM5 proteins form hexagonal nets on HIV-1 capsids. eLife. 2016; 5:e16269. [PubMed: 27253068]

Lima CD, Schulman BA. Structural biology: a protein engagement RING. Nature. 2012; 489:43–44. [PubMed: 22955611]

Liu HM, Loo YM, Horner SM, Zornetzer GA, Katze MG, Gale M Jr. The mitochondrial targeting chaperone 14-3-3ε regulates a RIG-I translocon that mediates membrane association and innate antiviral immunity. Cell Host Microbe. 2012; 11:528–537. [PubMed: 22607805]

Liu S, Chen J, Cai X, Wu J, Chen X, Wu YT, Sun L, Chen ZJ. MAVS recruits multiple ubiquitin E3 ligases to activate antiviral signaling cascades. eLife. 2013; 2:e00785. [PubMed: 23951545]

Loo YM, Gale M Jr. Immune signaling by RIG-I-like receptors. Immunity. 2011; 34:680–692. [PubMed: 21616437]

Luo D, Ding SC, Vela A, Kohlway A, Lindenbach BD, Pyle AM. Structural insights into RNA recognition by RIG-I. Cell. 2011; 147:409–422. [PubMed: 22000018]

Manokaran G, Finol E, Wang C, Gunaratne J, Bahl J, Ong EZ, Tan HC, Sessions OM, Ward AM, Gubler DJ, et al. Dengue subgenomic RNA binds TRIM25 to inhibit interferon expression for epidemiological fitness. Science. 2015; 350:217–221. [PubMed: 26138103]

Meroni G, Diez-Roux G. TRIM/RBCC, a novel class of 'single protein RING finger' E3 ubiquitin ligases. BioEssays. 2005; 27:1147–1157. [PubMed: 16237670]

Middleton AJ, Budhidarmo R, Day CL. Use of E2~ubiquitin conjugates for the characterization of ubiquitin transfer by RING E3 ligases such as the inhibitor of apoptosis proteins. Methods Enzymol. 2014; 545:243–263. [PubMed: 25065893]

Otwinowski Z, Minor W. Processing of X-ray diffraction data collected in oscillation mode. Methods Enzymol. 1997; 276:307–326. [PubMed: 27754618]

Peisley A, Wu B, Yao H, Walz T, Hur S. RIG-I forms signaling-competent filaments in an ATP-dependent, ubiquitin-independent manner. Mol Cell. 2013; 51:573–583. [PubMed: 23993742]

Peisley A, Wu B, Xu H, Chen ZJ, Hur S. Structural basis for ubiquitin-mediated antiviral signal activation by RIG-I. Nature. 2014; 509:110–114. [PubMed: 24590070]

Pichlmair A, Schulz O, Tan CP, Näslund TI, Liljeström P, Weber F, Reis e Sousa C. RIG-I-mediated antiviral responses to single-stranded RNA bearing 5′-phosphates. Science. 2006; 314:997–1001. [PubMed: 17038589]

Plechanovová A, Jaffray EG, Tatham MH, Naismith JH, Hay RT. Structure of a RING E3 ligase and ubiquitin-loaded E2 primed for catalysis. Nature. 2012; 489:115–120. [PubMed: 22842904]

Pruneda JN, Littlefield PJ, Soss SE, Nordquist KA, Chazin WJ, Brzovic PS, Klevit RE. Structure of an E3:E2~Ub complex reveals an allosteric mechanism shared among RING/U-box ligases. Mol Cell. 2012; 47:933–942. [PubMed: 22885007]

Rajsbaum R, Albrecht RA, Wang MK, Maharaj NP, Versteeg GA, Nistal-Villán E, García-Sastre A, Gack MU. Species-specific inhibition of RIG-I ubiquitination and IFN induction by the influenza A virus NS1 protein. PLoS Pathog. 2012; 8:e1003059. [PubMed: 23209422]

Sanchez JG, Okreglicka K, Chandrasekaran V, Welker JM, Sundquist WI, Pornillos O. The tripartite motif coiled-coil is an elongated antiparallel hairpin dimer. Proc Natl Acad Sci USA. 2014; 111:2494–2499. [PubMed: 24550273]

Wagner JM, Roganowicz MD, Skorupka K, Alam SL, Christensen DE, Doss GL, Wan Y, Frank GA, Ganser-Pornillos BK, Sundquist WI, Pornillos O. Mechanism of B-box 2 domain-mediated higher-order assembly of the retroviral restriction factor TRIM5α. eLife. 2016; 5:e16309. [PubMed: 27253059]

Weinert C, Morger D, Djekic A, Grütter MG, Mittl PR. Crystal structure of TRIM20 C-terminal coiled-coil/B30.2 fragment: implications for the recognition of higher order oligomers. Sci Rep. 2015; 5:10819. [PubMed: 26043233]

Wright JD, Mace PD, Day CL. Secondary ubiquitin-RING docking enhances Arkadia and Ark2C E3 ligase activity. Nat Struct Mol Biol. 2016; 23:45–52. [PubMed: 26656854]

Wu H. Higher-order assemblies in a new paradigm of signal transduction. Cell. 2013; 153:287–292. [PubMed: 23582320]

Wu B, Peisley A, Tetrault D, Li Z, Egelman EH, Magor KE, Walz T, Penczek PA, Hur S. Molecular imprinting as a signal-activation mechanism of the viral RNA sensor RIG-I. Mol Cell. 2014; 55:511–523. [PubMed: 25018021]

Xu H, He X, Zheng H, Huang LJ, Hou F, Yu Z, de la Cruz MJ, Borkowski B, Zhang X, Chen ZJ, Jiang QX. Structural basis for the prion-like MAVS filaments in antiviral innate immunity. eLife. 2014; 3:e01489. [PubMed: 24569476]

Yudina Z, Roa A, Johnson R, Biris N, de Souza Aranha Vieira DA, Tsi-person V, Reszka N, Taylor AB, Hart PJ, Demeler B, et al. RING dimerization links higher-order assembly of TRIM5α to synthesis of K63-linked polyubiquitin. Cell Rep. 2015; 12:788–797. [PubMed: 26212332]

Zeng W, Xu M, Liu S, Sun L, Chen ZJ. Key role of Ubc5 and lysine-63 polyubiquitination in viral activation of IRF3. Mol Cell. 2009; 36:315–325. [PubMed: 19854139]

Zeng W, Sun L, Jiang X, Chen X, Hou F, Adhikari A, Xu M, Chen ZJ. Reconstitution of the RIG-I pathway reveals a signaling role of unanchored polyubiquitin chains in innate immunity. Cell. 2010; 141:315–330. [PubMed: 20403326]
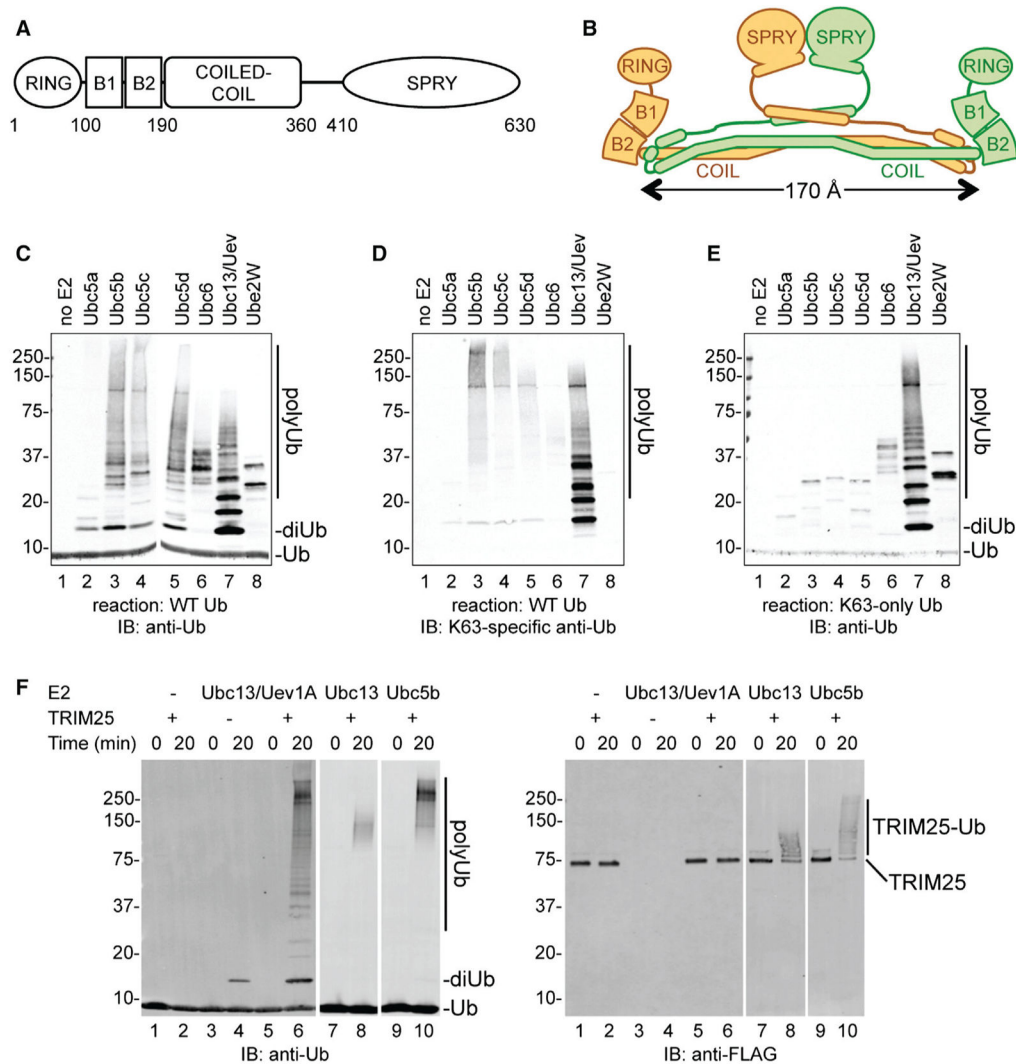
Figure 1. Primary Structure and E3 Ligase Activity of TRIM25

(A) Schematic of TRIM25 domain organization. Approximate amino acid boundaries of the different domains are indicated. B1, B-box 1; B2, B-box 2.

(B) Schematic of the elongated, antiparallel TRIM25 dimer, which places the catalytic RING domains around 170 Å apart. In this context, the RING domains are effectively monomeric.

(C) The isolated TRIM25 RING domain is active with Ubc5 isoforms and Ubc13/Uev1A. Purified RING (5 μM), E1 (50 nM), indicated E2s (1 μM), Ub (20 μM), and Mg-ATP (3 mM) were incubated at 37°C for 30 min. Ubiquitination products were observed by immunoblotting (IB) with anti-Ub antibody. Figure S1 shows the full screen of 26 different E2-conjugating enzymes, as well as a control experiment to confirm that chains made with Ubc13/Uev1A were not simply due to the known E3-independent activity of this heterodimeric E2.

(D) IB analysis, using K63-linkage specific anti-Ub, of the same samples in (C).

(E) The same reactions in (C) were performed but with K63-only Ub (wherein all Ub lysines except K63 are mutated to arginine). Only K63-linked polyUb chains are made in these reactions. IB was performed with anti-Ub.

(F) Full-length TRIM25 is active with Ubc5 and Ubc13/Uev1A. Reactions contained partially purified FLAG-tagged TRIM25 (200 nM) and either Ubc13/Uev1A (280 nM; lanes 1–6), Ubc13 alone (1 μM; lanes 7–8), or Ubc5b alone (1 μM; lanes 9–10). IB was performed with anti-Ub (left) or anti-FLAG (right). TRIM25 made only unanchored K63-linked polyUb with Ubc13/Uev1A but anchored (autoubiquitinated) Ub with Ubc13 alone or Ubc5b alone. However, faint di-Ub and tri-Ub bands can be discerned in the Ubc5 reactions at longer exposures of the anti-Ub blot.
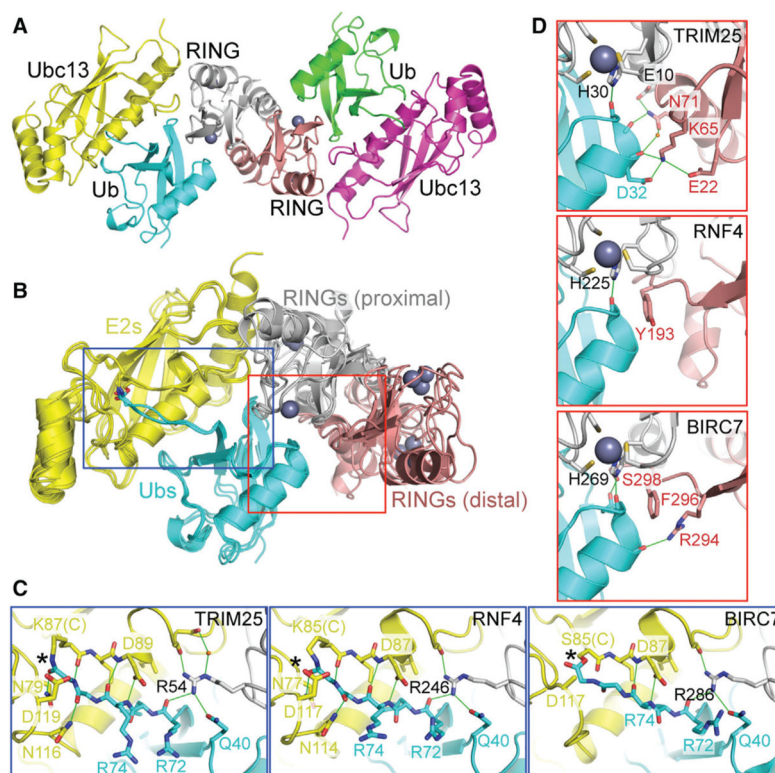
Figure 2. Structure of the TRIM25 RING Domain in Complex with Ub-Conjugated Ubc13

(A) The TRIM25 RING dimer is at the center of the complex, colored in gray and rose. Ubc13 molecules are colored in yellow and magenta. Ub molecules are colored in cyan and green. Zinc atoms are colored in gray. Structure statistics are in Table S1.

(B) Superposition of the TRIM25/Ubc13-Ub complex with the RNF4/Ubc5a-Ub complex (Plechanovová et al., 2012) and BIRC7/Ubc5a-Ub complex (Dou et al., 2012). Proximal and distal RING positions are defined relative to the bound Ub (cyan). Boxed regions are expanded in (C) (blue) and (D) (red).

(C) Details of the proximal RING interactions showing that the TRIM25 RING dimer (left) positions the Ub tail against the E2 in the same way as RNF4 (middle; Plechanovová et al., 2012) and BIRC7 (right; Dou et al., 2012). Landmark residues are shown as sticks and labeled. Asterisks indicate the covalent E2-Ub linkages (isopeptide in the TRIM25 and RNF4 complexes; oxyester in the BIRC7 complex). Hydrogen bonds are colored in green.

(D) Details of the distal RING interactions that help hold Ub in the "closed" position primed for catalysis. Also shown is a hydrogen bond between the zinc-coordinating His30 side chain in the proximal TRIM25 RING and Ub Glu24 carbonyl (top panel). Both RNF4 (middle; Plechanovová et al., 2012) and BIRC7 (bottom; Dou et al., 2012) make equivalent interactions.
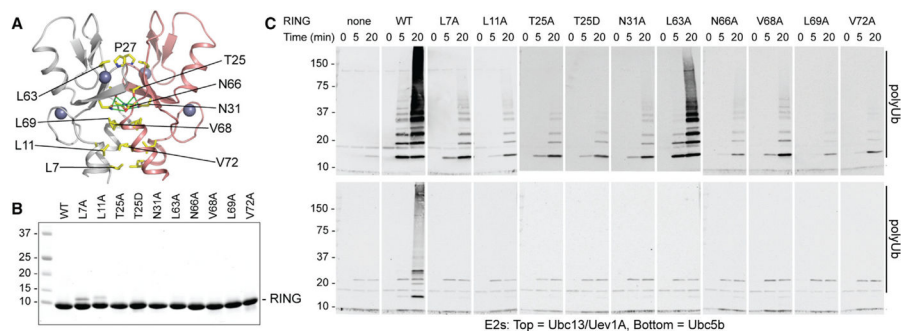
Figure 3. Structure-Based Mutagenesis of the TRIM25 RING Dimer Interface

(A) The TRIM25 RING dimer is stabilized by a buried network of hydrogen bonds (green lines) between the two zinc lobes and by a four-helix bundle made by residues that flank the zinc lobes in primary sequence. Residues in close contact within the dimer interface are shown as sticks and labeled.

(B) Coomassie-stained SDS-PAGE gel of purified WT and mutant recombinant RING proteins. See also Figure S3.

(C) Ubiquitination activities of the RING mutants (5 μM) with Ubc13/Uev1A (250 nM; top panels) or Ubc5b (1 μM; bottom panels). Samples were analyzed by IB with anti-Ub.
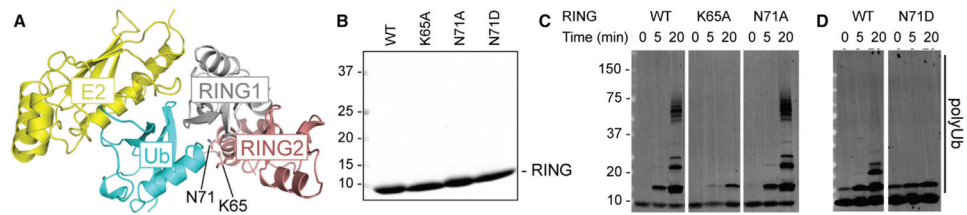
Figure 4. The Non-conserved Second Set of RING/Ub Interactions Is Required for Catalysis

(A) Location of Asn71 and K65 (sticks) in context of the complex.

(B) Coomassie-stained SDS-PAGE gel of purified WT and mutant recombinant RING proteins. See also Figure S3.

(C and D) Ubiquitination assays with indicated RING mutants (5 μM) and Ubc13/Uev1A (250 nM). WT panels show corresponding control experiments, performed in parallel. Samples were analyzed by IB with anti-Ub.
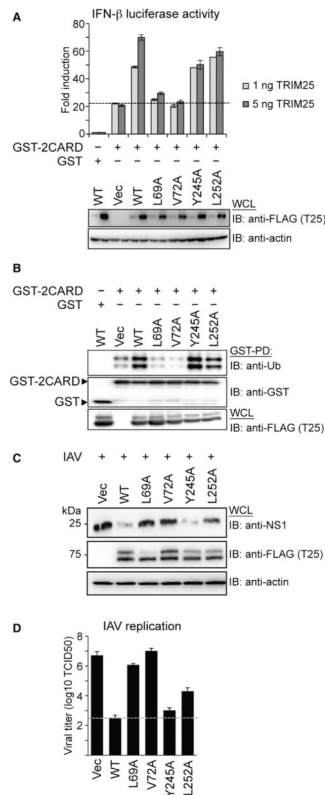
Figure 5. IFN Induction, Ubiquitination, and Antiviral Activities of TRIM25

(A) IFN-β induction by WT and TRIM25 mutants. *TRIM25*-KO HEK293T cells (Figure S4) were transfected with plasmids encoding IFN-β-luciferase, β-galactosidase, GST, or GST-2CARD and empty vector (Vec) or the indicated FLAG-tagged TRIM25 (T25) constructs (see Experimental Procedures for details). Twelve hours later, IFN-β promoter activity was measured by a luciferase assay and values were normalized to β-galactosidase. Whole-cell lysates (WCLs) were analyzed by IB with the indicated antibodies. Results are expressed as mean ± SD (n = 2).

(B) Ubiquitination of RIG-I 2CARD. *TRIM25*-KO HEK293T cells were transfected with plasmid for GST or GST-2CARD, together with Vec or the indicated FLAG-TRIM25 constructs. Forty-eight hours later, cells were lysed and WCLs subjected to GST pull-down (GST-PD), followed by IB with anti-Ub and anti-GST antibodies. IB of WCLs was performed with anti-FLAG antibody to determine the expression levels of the TRIM25 WT and mutant proteins.

(C and D) Replication of influenza A virus (IAV) (H1N1 PR8 strain) in *TRIM25*-KO HEK293T cells reconstituted with TRIM25 WT or mutants. Cells were transfected with Vec or plasmids encoding FLAG-tagged TRIM25 WT or the indicated mutants. At 24 hr post-transfection, cells were infected with IAV (MOI 0.01) for 96 hr. Expression levels of IAV NS1, actin, and TRIM25 constructs were analyzed by IB with anti-NS1, anti-actin, and anti-FLAG (TRIM25) antibodies (C). IAV titers in the supernatant of reconstituted *TRIM25*-KO cells were determined by TCID50 assay (D). The results shown are from two independent experiments.
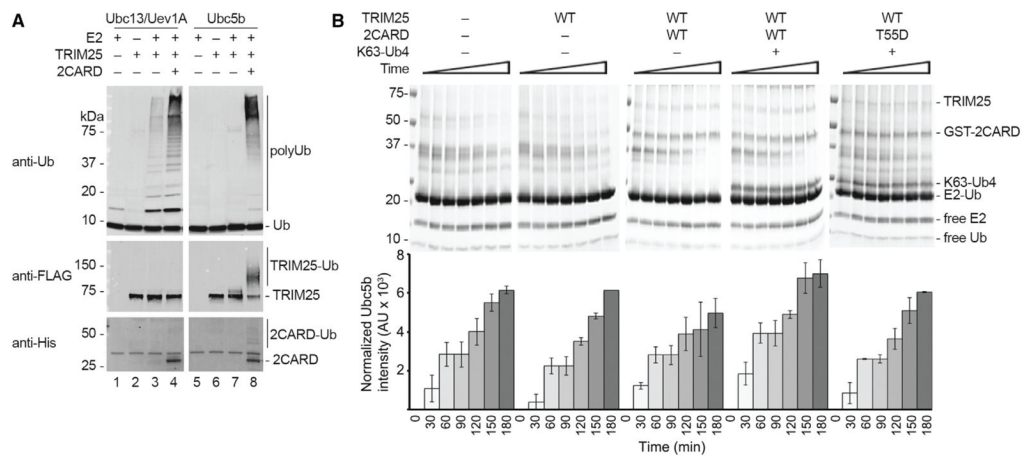
Figure 6. RIG-I 2CARD Enhances TRIM25's Catalytic Activity In Vitro

(A) Ubiquitination activity of 100 nM FLAG-TRIM25 in the presence or absence of His-tagged RIG-I 2CARD. Reaction mixtures were analyzed by IB with anti-Ub (top), anti-FLAG (middle), and anti-His (bottom). As with the autoubiquitination reactions, substrate-attached Ub was observed only with Ubc5b and not with Ubc13/Uev1A. This experiment was performed with five independent protein preparations, with similar results.

(B) Oxyester hydrolysis assays showing the disappearance of Ubc5b$^{S22R/C85S}$-Ub conjugates and the appearance of free Ubc5b in the presence of full-length TRIM25 (1 μM), GST-tagged WT or T55D RIG-I 2CARD (8 μM), and/or K63-linked tetraUb (5 μM) over 180 min. (Top) Samples were resolved by using non-reducing SDS-PAGE and Coomassie blue staining. Experiments were performed in duplicate, and one set is shown. (Bottom) Densitometry quantification of gels follows the appearance of free Ubc5b over time. Error bars show the range values obtained in two independent experiments, performed with independent protein preparations of both TRIM25 and 2CARD.
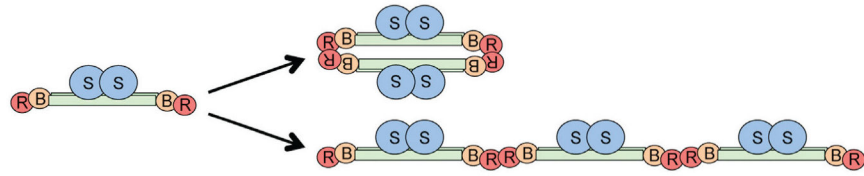
Figure 7. TRIM25 RING Dimerization
Shown are two possible modes of higher-order assembly of coiled-coil-mediated TRIM25 protein dimers that will promote RING/RING dimerization. The domains are color-coded as follows: red, RING (R); orange, B-boxes (B); green, coiled coil; blue, SPRY (S).